Subsolidus phase equilibria in the RuO_2–Bi_2O_3–SiO_2 system

Marko Hrovat, Thomas Maeder[*] Janez Holc, Darko Belavič[**], Jena Cilenšek and Janez Bernard[***]

Jožef Stefan Institute, Jamova 39, SI-1000 Ljubljana, Slovenia
[*] Ecole Polytechnique Federale de Lausanne, CH-1015, Lausanne, Switzerland
[**] HIPOT-R&D, d.o.o., Trubarjeva 7, SI-8310 Sentjernej, Slovenia
[***] Slovenian National Building and Civil Engineering Institute, Dimičeva 12, SI-1000 Ljubljana, Slovenia

Corresponding author (Marko Hrovat)
Tel. +386 1 477 3900
Fax. +386 1 477 3887
e-mail: marko.hrovat@ijs.si

Abstract

Subsolidus equilibria in the RuO_2–Bi_2O_3–SiO_2 diagram were studied with the aim of investigating possible interactions between the bismuth-ruthenate-based conductive phase and the silica-rich glasses in thick-film resistors. The tie lines are between $Bi_2Ru_2O_7$ and $Bi_{12}SiO_{20}$ (gamma phase), between $Bi_2Ru_2O_7$ and $Bi_4Si_3O_{12}$, and between RuO_2 and $Bi_4Si_3O_{12}$. This indicates that the bismuth ruthenate is not stable in the presence of the silica-rich glass phase.

Keywords: B X ray methods, B electron microscopy, phase equlibria

Introduction

Thick-film resistor pastes consist basically of a conducting phase, a lead-borosilicate-based glass phase and an organic vehicle that burns out during high-temperature processing. In most modern thick-film resistor compositions the conductive phase is either RuO_2 or ruthenates; mainly bismuth ($Bi_2Ru_2O_7$) or lead ($Pb_2Ru_2O_6$) ruthenates. During the firing cycle all the constituents of the resistor paste react with each other and the melted glass also interacts with the substrate. The resistors are only a relatively short time (typically 10 min) at the highest temperature (typically 850^{o}C). Because of this the reactions between the main constituents (the glass and the conductive phase) of the resistor material do not reach equilibrium ([1-4]).

If thick-film resistors are fired at temperatures higher than the required 850^{o}C, and for a relatively long time, the interactions between the conductive phase and the lead-borosilicate-based glass phase that is rich in silica approach equilibrium. This tends to decrease the sheet resistivities and increase the temperature coefficients of resistivity (TCRs) of these "overfired" resistors ([5-7]). The X-ray diffraction (XRD) spectra of bismuth-ruthenate-based "equilibrated" resistors showed that at higher firing temperatures the ruthenate decomposes, forming RuO_2, while the conductive phase in RuO_2-based resistors stays unchanged. This is shown in Fig. 1 for 10 kohm/sq. DuPont 8039 and DuPont 8041 thick-film resistors. The 8039 material is based on $Bi_2Ru_2O_7$ and the 8041 material is based on RuO_2 ([4]). The spectra of bismuth ruthenate (denoted RU) and of RuO_2 (denoted RuO2) are included. The resistors were fired for 10 min at 850^{o}C and for 3 hours at 950^{o}C. After 3 hours of firing at 950^{o}C the ruthenate peaks of the 8039 resistors disappear, while the spectrum of 8041 fired under the same conditions remains more or less unchanged.

Likewise, the decomposition of $Bi_2Ru_2O_7$ was reported for lead-free silica-based glasses at "normal" firing temperatures and times at peak temperatures. ([8]).

Presumably because of the interaction with the molten glass, the bismuth ruthenate decomposed into Bi_2O_3, which is dissolved in the glass, and into RuO_2. Adachi and Kuno ([9,10]), for example, studied (in a similar system) high-temperature interactions between $PbO–B_2O_3–SiO_2$ glasses and $Pb_2Ru_2O_{6.5}$ or RuO_2. They showed that in

glasses "poor" in PbO the $Pb_2Ru_2O_{6.5}$ disappears and RuO_2 is formed, while for PbO-rich glasses the RuO_2 reacts with the PbO from the glass and forms $Pb_2Ru_2O_{6.5}$. The reactions between lead ruthenate and silica-rich glasses were confirmed by Hrovat et al ([11]).

Recently, due to environmental concerns and the corresponding European RoHS directive ([12]), there has been a strong drive towards removing lead from thick-film materials. While glasses in electronics (and hence resistors) currently benefit from an exemption ([13]), lead-free materials clearly have favour among customers. To address this concern, thick-film suppliers have progressively introduced lead-free conductors, dielectrics and overglazes.

For resistors and overglazes, which need relatively low-melting glasses, the obvious replacement for PbO is the much less toxic Bi_2O_3, for the following reasons. First, Bi-based glasses are very similar to Pb-based ones ([14-15]) in processing and flowability, due to the similarity of the polarizable Pb^{2+} and Bi^{3+} ions. Also, Bi_2O_3 has already for a long time been in wide use in thick-film electronics, as an adhesion / solderability promoter in conductors (alone or in glasses) and in the bismuth ruthenate used in many resistive compositions ([4, 16]). Bi_2O_3 can also be added to resistors, to their terminations and/or to the underlying dielectrics to tune the properties and improve materials compatibility ([17]). In fact, Bi-based overglazes are commercially available. However, because of the complex chemical interactions in resistive materials ([1-4]), lead has been difficult to replace altogether in thick-film resistors, although lead-free compositions with Bi-based glasses (30-70 wt% Bi) and Ru-based conductive materials have already been patented a long time ago ([18]), without discussion of the phase evolution. More recently, similar lead-free resistors have been proposed ([19]) with RuO_2 as a conductive phase and a glass having a relatively low Bi content, ca. 20 wt% ([20]). In this case, the phase evolution was investigated: no bismuth ruthenate formed upon firing, which can be ascribed to the low Bi content of the glass, by analogy to the results of Adachi and Kuno with Pb ruthenate and Pb-conducting glass ([9-10]).

From the above considerations, studying and understanding the phase relations between Bi-containing glasses, RuO_2 and $Bi_2Ru_2O_7$ (in pure form or partly

substituted) is of prime importance for the development of lead-free resistors. As a contribution to this topic, the aim of this work was to investigate subsolidus phase equilibria (in air) in the RuO_2–Bi_2O_3–SiO_2 system.

Phase equilibria in the RuO_2–Bi_2O_3 system were studied by Hrovat et al. ([20]). The binary $Bi_2Ru_2O_7$ compound decomposes above 1200°C into Bi_2O_3 and RuO_2. The eutectic composition is around 80% Bi_2O_3, and the eutectic temperature is 745°C. In the RuO_2–SiO_2 system there is no binary compound and no liquid phase (eutectic) up to 1405°C, the temperature at which RuO_2 decomposes (in air) to metallic ruthenium and oxygen ([11]).

In the Bi_2O_3–SiO_2 system are two binary compounds: $Bi_{12}SiO_{20}$ (with a SiO_2-stabilised Bi_2O_3 gamma phase) and $Bi_4Si_3O_{12}$ ([21,22]). The eutectic temperatures are at 810°C, between Bi_2O_3 and the gamma phase; at 870°C, between the gamma phase and $Bi_4Si_3O_{12}$; and at 950°C, between $Bi_4Si_3O_{12}$ and SiO_2. Kettner and Kramer ([23]) characterised another binary compound in this system, i.e., Bi_2SiO_5. This compound was formed during the long-term (five days at 670°C) synthesis of $PbBiO_2Cl$ in closed quartz ampoules by a reaction between incipient chemicals and the quartz wall of the ampoule.

Experimental

For the experimental work, RuO_2 (Ventron, 99.9%), Bi_2O_3 (Johnson Matthey, 99.99%), and SiO_2 (Riedel de Haen, 99.9%) were used. The oxides were mixed in isopropyl alcohol, pressed into pellets, and fired up to five times in air at 750°C with intermediate grinding. During firing the pellets were placed on platinum foils. The compositions of the relevant samples in the RuO_2–Bi_2O_3–SiO_2 system can be related to Fig. 4.

The fired materials were characterised as powders by X-ray powder diffraction analysis using a Philips PW 1710 X-ray diffractometer with Cu Kα radiation. X-ray spectra were measured from $2\Theta = 20^o$ to $2\Theta = 70^o$ in steps of 0.02^o. A JEOL 5800

scanning electron microscope (SEM) equipped with a link ISIS 300 energy-dispersive X-ray analyser (EDS) was used for the overall microstructural and compositional analysis. Samples prepared for the SEM were mounted in epoxy in a cross-sectional orientation and then polished using standard metallographic techniques. Prior to analysis in the SEM, the samples were coated with carbon to provide electrical conductivity and to avoid charging effects. The microstructures of the polished samples were studied by back-scattered electron imaging using compositional contrast to distinguish between the phases that differ in density (average atomic number Z).

Results and discussion

The results of the X-ray powder analysis of the relevant samples, fired in air at 750^{o}C, are summarised in Table 1. The nominal compositions of the samples and the phases identified after firing are presented. An example of XRD spectrum (Sample 10 in Tbla 1, 2 Bi_2O_3 + 4 RuO_2 + 3 SiO_2) after firing is shown in Fig.2. Peaks of Peaks of RuO_2 are denoted as R and peaks of $Bi_4Si_3O_{12}$ are denoted BS.

Table 1. Results of the X-ray diffraction analysis of some compositions in the RuO_2–Bi_2O_3–SiO_2 system, fired in air at 750°C

Sample	Nominal composition	Phases identified
1	$Bi_2O_3 + 3\ SiO_2$	$Bi_4Si_3O_{12} + SiO_2$
2	$2\ Bi_2O_3 + 3\ SiO_2$	$Bi_4Si_3O_{12}$
3	$3\ Bi_2O_3 + 2\ SiO_2$	$Bi_4Si_3O_{12} + Bi_{12}SiO_{20}$ (gamma phase)
4	$6\ Bi_2O_3 + SiO_2$	$Bi_{12}SiO_{20}$ (gamma phase)
5	$Bi_2O_3 + 2\ RuO_2$	$Bi_2Ru_2O_7$
6	$6\ Bi_2O_3 + 2\ RuO_2 + SiO_2$	$Bi_2Ru_2O_7 + Bi_{12}SiO_{20}$ (gamma phase)
7	$7\ Bi_2O_3 + 3\ RuO_2 + 3\ SiO_2$	$Bi_2Ru_2O_7 + Bi_{12}SiO_{20}$ (gamma phase) + $Bi_4Si_3O_{12}$
8	$3\ Bi_2O_3 + 2\ RuO_2 + 3\ SiO_2$	$Bi_2Ru_2O_7 + Bi_4Si_3O_{12}$
9	$Bi_2O_3 + 2\ RuO_2 + SiO_2$	$Bi_2Ru_2O_7 + RuO_2 + Bi_4Si_3O_{12}$
10	$2\ Bi_2O_3 + 4\ RuO_2 + 3\ SiO_2$	$RuO_2 + Bi_4Si_3O_{12}$
11	$5Bi_2O_3 + 22RuO_2 + 8SiO_2$	$RuO_2 + Bi_4Si_3O_{12}$
12	$Bi_2O_3 + 2\ RuO_2 + 4\ SiO_2$	$RuO_2 + Bi_4Si_3O_{12} + SiO_2$
13	$2\ Bi_2O_3 + 4\ RuO_2 + 4\ SiO_2$	$RuO_2 + Bi_4Si_3O_{12} + SiO_2$

The microstructures of the materials with the nominal compositions $3\ Bi_2O_3 + 2\ SiO_2$ and $Bi_2O_3 + 2\ RuO_2 + 4\ SiO_2$ are shown in Figs. 2 and 3, respectively. The first microstructure is a two-phase mixture of the light $Bi_{12}SiO_{20}$ gamma phase and the grey $Bi_4Si_3O_{12}$ phase. Fig. 3 is a three-phase mixture of the SiO_2 dark phase, small grey RuO_2 particles and the lighter $Bi_4Si_3O_{12}$ phase.

Based on the results obtained by XRD and EDS, a proposed subsolidus RuO_2–Bi_2O_3–SiO_2 diagram, shown in Fig. 4, was constructed. The compositions of the relevant samples are denoted by circles. No ternary compound was found. The tie lines are between $Bi_2Ru_2O_7$ and $Bi_{12}SiO_{20}$, between $Bi_2Ru_2O_7$ and $Bi_4Si_3O_{12}$, and between RuO_2 and $Bi_4Si_3O_{12}$. The Bi_2SiO_5 compound in the Bi_2O_3–SiO_2 system, reported by Kettner and Kramer ([23]), was not found either by X-ray or EDS analysis, and it could therefore be assumed that it could not be formed under the described synthesis conditions. The results (the tie line between RuO_2 and $Bi_4Si_3O_{12}$) therefore

indicate that the bismuth-ruthenate-based conductive phase in thick-film resistors is unstable when in contact with the SiO_2. This could also explain results reported by Morten et al. ([8]) who reported the compatibility of RuO_2 and the incompatibility of $Bi_2Ru_2O_7$ with lead-free silica rich glasses.

Conclusions

After long-term high-temperature firing the conductive phase in thick-film resistors based on RuO_2 remains unchanged. In contrast, the $Bi_2Ru_2O_7$ decomposed, presumably due to interactions with the silica-rich glass phase. Subsolidus equilibria in the RuO_2–Bi_2O_3–SiO_2 diagram were studied by X-ray powder diffraction analysis and energy-dispersive X-ray analysis. The aim was to investigate possible interactions between the conductive phase (either ruthenium oxide or bismuth ruthenate) and silica-rich glasses in either leaded or lead-free thick-film resistors. No ternary compound was found in the system. The tie lines are between $Bi_2Ru_2O_7$ and $Bi_{12}SiO_{20}$, between $Bi_2Ru_2O_7$ and $Bi_4Si_3O_{12}$, and between RuO_2 and $Bi_4Si_3O_{12}$. This indicates that the bismuth ruthenate is not compatible with the silica rich glass phase.

Acknowledgement

The financial support of the Slovenian Research Agency is gratefully acknowledged.

References

1. J. W. Pierce, D. W. Kuty, J. L. Larry, The chemistry and stability of ruthenium based resistors, Solid State Technol., 25, (10), (1982), 85-93
2. T. Inokuma, Y. Taketa, "Control of electrical properties of RuO_2 thick film resistors", Active and Passive Elect. Comp., 12, (3), (1987), 155-166
3. O. Abe, Y. Taketa, M. Haradome, The effect of various factors on the resistivity and TCR of RuO_2 thick film resistors - relation between the electrical properties and particle size of constituents, the physical properties of glass and firing temperature, Active and Passive Elect. Comp., 13, (2), (1988), 76-83
4. M. Hrovat, Z. Samardžija, J. Holc, D. Belavič, Microstructural, XRD and electrical characterization of some thick film resistors, J. Mater. Sci.: Materials in Electronics, 11, (3), (2000), 199-208
5. D. Boffeli, E. Broitman, R. Zimmerman. Resistance adjustment in RuO_2 based thick film strain gauges by laser irradiation, J. Mater. Sci. Lett., 16, (1997), 1983-1985
6. M. Hrovat, A, Benčan, D. Belavič, J. Holc, G. Dražić, The influence of firing temperature on the electrical and microstructural characteristics of thick film resistors for strain gauge applications, Sens. Actuators A, Phys.., 103, (2003), 341-352
7. M. Hrovat, D. Belavič, A. Benčan, J. Holc, G. Dražič, A characterization of thick-film PTC resistors, Sensors Actuators A, 117, (2), (2005), 256-266
8. B. Morten, G. Ruffi, F. Sirotti, A. Tombesi, L. Moro, T. Akomolafe, Lead-free ruthenium-based thick-film resistors: a study of model systems, J. Mater. Sci.: Materials in Electronics, 2, (1), (1991), 46-53
9. K. Adachi, H. Kuno, Decomposition of ruthenium oxides in lead borosilicate glass, J. Am. Ceram. Soc., 80, (5), (1997), 1055-1064
10. K. Adachi, H. Kuno, Effect of glass composition on the electrical properties of thick film resistors, J. Am. Ceram. Soc., 83, (10), (2000), 2441-2448
11. M. Hrovat, J. Holc, D. Belavič. J. Bernard, Subsolidus phase equilibria in the PbO poor part of RuO_2-PbO-SiO_2 system, Materials Letters, 60, (20), (2006), 2501-2503

12. On the restriction of the use of certain hazardous substances in electrical and electronic equipment (ROHS), directive 2002/95/EC of the European Parliament and of the Council, 2002.
13. Frequently asked questions on directive 2002/95/EC on the restriction of the use of certain hazardous substances in electrical and electronic equipment (RoHS) and directive 2002/96/EC on waste electrical and electronic equipment (WEEE), European Commission, Directorate-General Environment, 2006.
14. S.M. Brekhovskikh, Glasses with high bismuth and lead contents, Glass and Ceramics 14 (8), 264-267, 1960.
15. G.E. Rachkovskaya, G.B. Zakharevich, "Properties, structure, and application of low-melting lead–bismuth glasses", Glass and Ceramics 61 (1-2), 9-12, 2004.
16. M. Monneraye, "Les encres sérigraphiables en microélectronique hybride: les matériaux et leur comportement (Screenable inks in hybrid microelectronics: the materials and their behaviour), Acta Electronica 21 (4), 263-281, 1978.
17. C. Jacq, T. Maeder, N. Johner-N Corradini-G Ryer-P, "High performance low-firing temperature thick-film pressure sensors on steel", Proceedings, 16th IMAPS - EMPC, Oulu, Finnland, 167-170, 2007.
18. J. Hormadaly, "Cadmium-free and lead-free thick film paste composition", United States Patent 5’491’118, 1996.
19. M.G. Busana, M. Prudenziati, J. Hormadaly, "Microstructure development and electrical properties of RuO_2-based lead-free thick film resistors", Journal of Materials Science: Materials in Electronics, Vol. 17, 951-962, 2006.
20. M. Hrovat, S. Bernik, D. Kolar, Phase equilibria in the $RuO_2 – Bi_2O_3 – PdO$ system, J. Mater. Sci. Lett., 7, (6), (1988), 637-962-638
21. E. M. Levin, R. S. Roth, Polymorphism of bismuth sesquioxide. II. Effects of oxide addition on the polymorphism of Bi_2O_3, J. Res. Nat. Bur. Stand., 68 A, (2), (1964), 197-206
22. V. M. Skorikov, P. F. Rza-Zade, Y. F. Kargin, F. F. Dzhalaladdinov, Phase equilibria in the $Ga_2O_3 – Bi_2O_3 – EO_2$ (where E – Si and Ge), Zh. Neorg. Khim., 26, (4), (1981), 1070-1074 (in Russian) – (Engl. Transl.) Russ. J. Inorg. Chem., 26, (4), (1981), 581-584
23. J. Ketterer, V. Kramer, Crystal structure of the bismuth silicate Bi_2SiO_5, N. Jb. Miner. Mh., 1, (1986), 13-18

Figure captions

Fig. 1.a: X-ray spectra of Du Pont thick-film resistors 8039 fired for 10 min at 850°C and for 3 hours at 950°C. The material is based on $Bi_2Ru_2O_7$. Spectra of bismuth ruthenate (denoted RU) and of RuO_2 (denoted RuO2) are included. Peaks of $SiZrO_3$ are denoted by asterisks.

Fig. 1.b: X-ray spectra of Du Pont thick-film resistors 8041 fired for 10 min at 850°C and for 3 hours at 950°C. The material is based on RuO_2. Spectra of bismuth ruthenate (denoted RU) and of RuO_2 (denoted RuO2) are included.

Fig 2: X-ray spectra of $2Bi_2O_3 + 4\ RuO_2 + 3\ SiO_2$ (sample 10 in Table 1) fired at 750°C. Peaks of RuO_2 are denoted as R and peaks of $Bi_4Si_3O_{12}$ are denoted BS.

Fig. 3 Microstructure (backscattered electrons) of the sample with the nominal composition $3\ Bi_2O_3 + 2\ SiO_2$. The material is a two-phase mixture of the light $Bi_{12}SiO_{20}$ gamma phase and the grey $Bi_4Si_3O_{12}$ phase.

Fig. 4: Microstructure (backscattered electrons) of the sample with the nominal composition $Bi_2O_3 + 2\ RuO_2 + 4\ SiO_2$. The material is a three-phase mixture of the SiO_2 dark phase, small grey RuO_2 particles and the lighter $Bi_4Si_3O_{12}$ phase.

Fig. 5: A proposed subsolidus RuO_2–Bi_2O_3–SiO_2 diagram. The compositions of the relevant samples are denoted by circles. The tie lines are between $Bi_2Ru_2O_7$ and $Bi_{12}SiO_{20}$, between $Bi_2Ru_2O_7$ and $Bi_4Si_3O_{12}$, and between RuO_2 and $Bi_4Si_3O_{12}$.

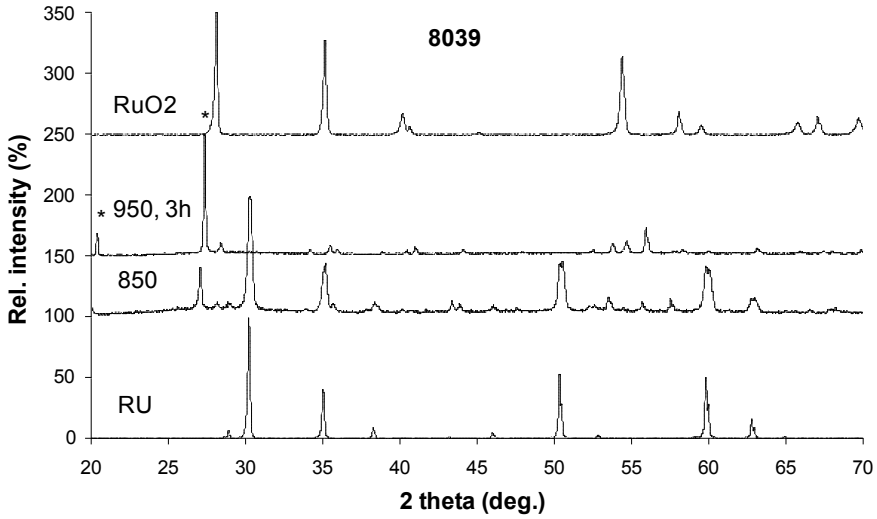
8039
RuO2
*
* 950, 3h
850
RU
Rel. intensity (%)
2 theta (deg.)
350
300
250
200
150
100
50
0
20
25
30
35
40
45
50
55
60
65
70

Fig. 1.a

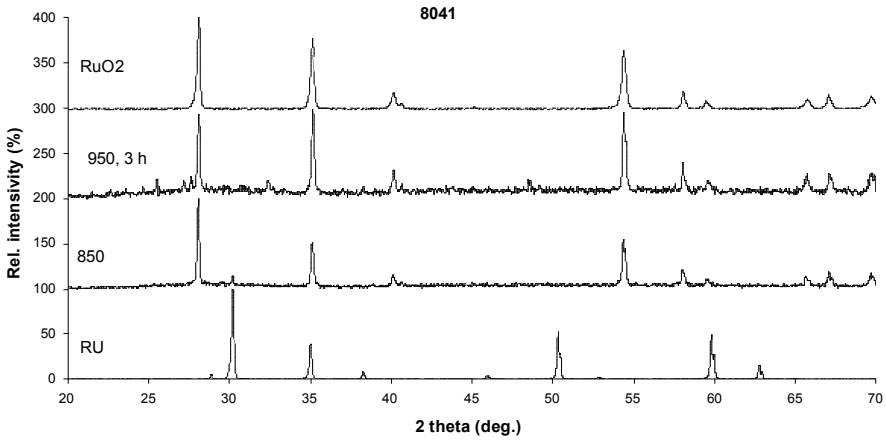
8041
RuO2
950, 3 h
850
RU
Rel. intensivity (%)
2 theta (deg.)
0
50
100
150
200
250
300
350
400
20
25
30
35
40
45
50
55
60
65
70

Fig. 1.b

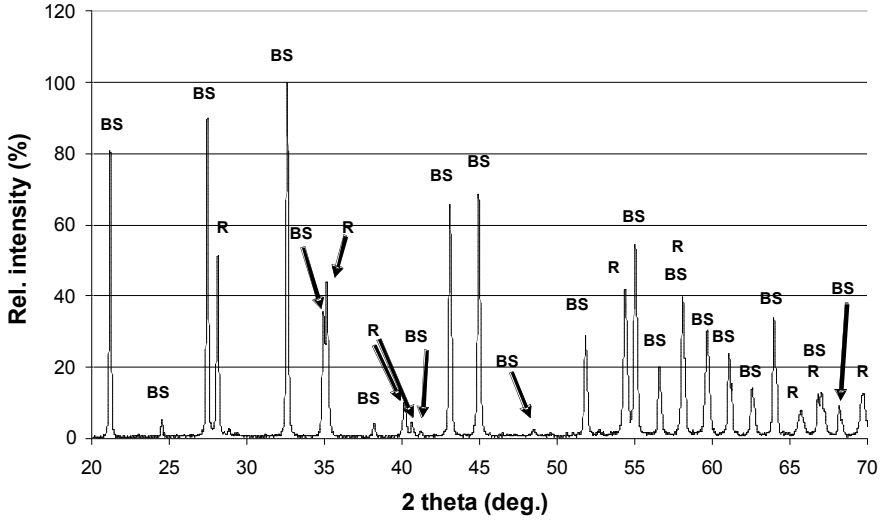

Fig. 2

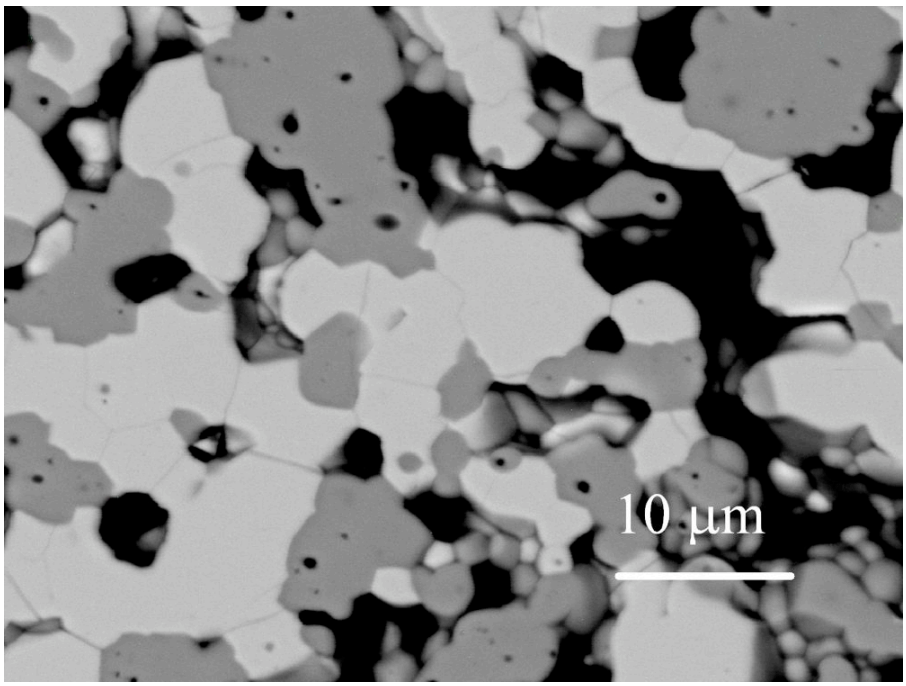

Fig. 3

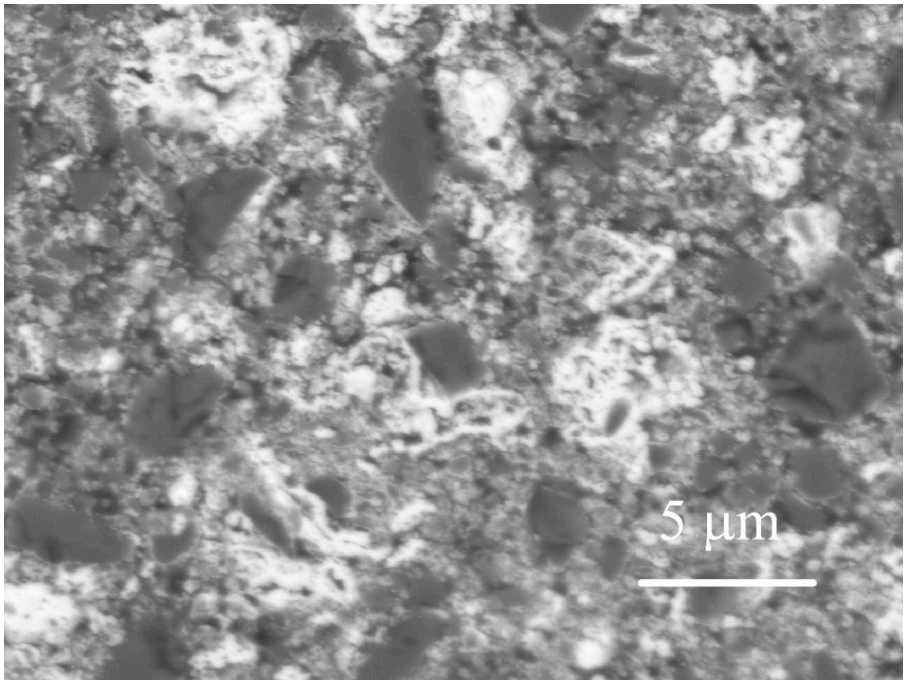

Fig. 4

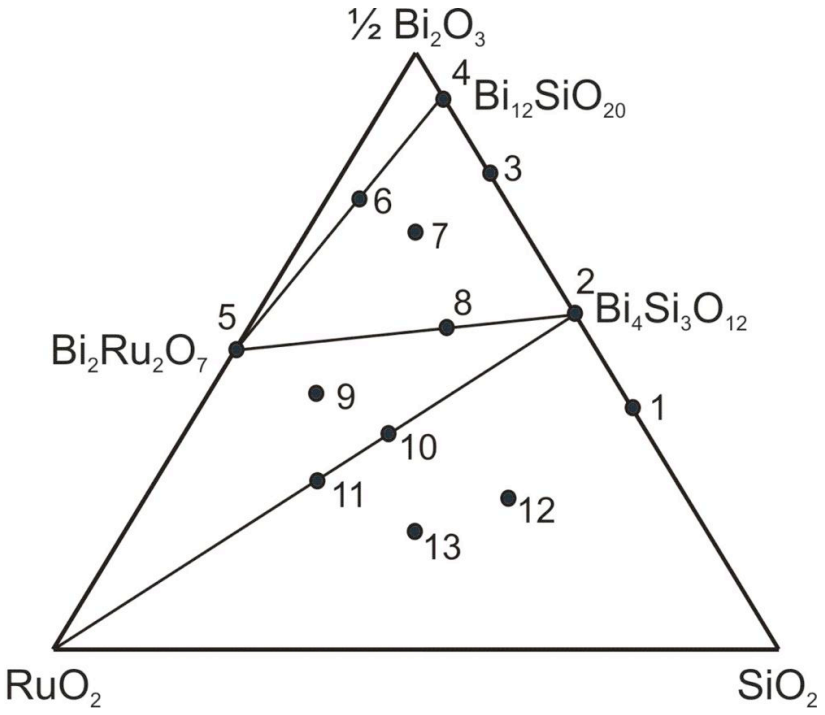
½ Bi2O3
4
Bi12SiO20
3
6
7
2
Bi4Si3O12
5
8
Bi2Ru2O7
9
1
10
11
12
13
RuO2
SiO2

Fig. 5